Yamunadhari Kumar 2021, 9:6
ISSN (Online): 2348-4098
ISSN (Print): 2395-4752

Power Quality Improvement in a Grid Connected Hybrid Energy Generation System Using UPFC

Research Scholar Yamunadhari Kumar, Prof. Mamta Sood, Dr. Manju Gupta
Dr. Anuprita Mishra
Department of Electrical and Electronics Engineering
Oriental Institute of Science & Technology Bhopal, India
yamuna1992dhari@gmail.com,mamta_sood@oriental.ac.in,manjugupta@oriental.ac.in, anupritamishra@oriental.ac.in.

Abstract-Energy production and transmission have had to increase ruthlessly in recent years due to resource and environmental constraints, while demand for electric power has surged significantly. As a result of several transmission lines being substantially loaded, power system stability became a limiting factor in electric power transmission. It's vital to keep the electrical grid safe and stable, thus it's not a simple assignment. The FACTs devices are used to manage power and attenuate oscillations. This study explains how to use MATLAB Simulink to benefit from the modified particle swarm optimization (PSO) approach to better stabilize MPPT with UPFC by employing the PI-C and MATLAB Simulink parameters that build optimal proportional integral controllers. When a power system failure occurs, the UPFC investigates by emulating the power system's operating characteristics using the two recommended approaches. When compared to existing techniques, the proposed PSO technically improves the system's reactivity and reduces the amount of undershoot and overshoot in transitions. The results suggest that using this strategy significantly enhanced the simulation model's transient stability.

Index Terms- Microgrids (MGs), unified power flow controller (UPFC), Partical swarm optimization (PSO), proportional-integral-derivative (PID) Controller, Solar, Wind Turbine, Battery, Fuel Cell.

I. INTRODUCTION

Renewable energy is power derived from natural possessions, such as solar, wind, waves, or geothermal energy. Therefore, compared to the depletion of traditional fossil fuels [1], these sources of information are considered inexhaustible. The global power crunch provides a new impetus for the development or maturity of clean or renewable energy. [2]. In addition to the decline in fossil fuel transportation worldwide, another major reason fossil fuels do not work is the pollution associated with burning fossil fuels. In contrast, it is well known that compared to traditional energy sources, renewable energy sources are cleaner, or energy produced has no adverse effects on pollution.

comes from renewable or non-renewable energy sources. The current is then transmitted from one place to another through the transmission line. Finally, the power is distributed among the users using distribution feeders. A micro-grid is defined as a "local grid that connects distributed energy sources with organized loads and is usually connected to the traditional central grid synchronously" [17].

All of these sources are categorized as "micro-resources," which include lithium-ion batteries and solid oxide fuel cells. As a result, each source is limited in terms of how it can be linked to the distribution system. The power supply to the circulated network is met by the micro-power source and the mains, and the load is connected to the distributed network.

In the event of a mains failure, disconnect the MG from the mains on the PCC by operating a switch that separates the MG from the mains. After disconnection from the mains, the MG will work solely according to a predefined control strategy and supply power to the load by gradually increasing the power provided by all micro-sources. In this way, the load can be turned on, even during a power failure.

If the load requirement exceeds the micro-source capacity in island mode, some non-emergency loads can be disconnected. Maintain mains voltage and frequency by operating at least one converter under V / f control. After troubleshooting, only when the voltage error is less than 3%, the frequency error is less than 0.1 Hz, or the phase angle error is less than 100 can MG be reconnected to the mains [3].

II. RELATED WORK

Hamache (2019) et.al this article synthesizes a UPFC (unified power flow controller) device controller using the Decentralized Discrete Time Quasi Sliding Mode Control (DDTQSMC) technique to track actual and reactive power references over an EHV link. The DDTQSMC control intends to improve on existing linear continuous controls in terms of durability and transient precision. This application makes use of discrete state dynamics and a discrete sliding mode approach developed at UPFC.

Before building the DDTQSMC controller, which employs plant dynamics and discrete time sliding mode theory, a discrete state space model of the UPFC's dynamic behavior is required. Numerical simulation reveals that the suggested controller is accurate, effective, and long-lasting when utilized to direct an EHV interconnection using the DDTQSMC approach.

P. Rajivgandhi (2019) et.al Transmission networks are critical in regulating the amount of reactive power in a utility grid that supplies energy to a system. With the advancement of wind storage technology, wind-connected turbines will be required to generate reactive power during periods of high demand as well as under temporary conditions. Production of reactive power. This study investigates the effect of UPFC modulation on wind power system strength.

To ensure the UPFC's efficacy in regulating the wind resource utility grid system, component tuning of the UPFC compensators is critical in the regularization process. For the first time, the DFIG system is detailed in detail in this publication. Following that, UPFC-connected systems, as well as wind farms and electrical grids, are explored.

As a result, the compensation technique for the UPFC network's Levy fly Gray wolf optimizer is clarified. Finally, methods for regulating reactive and true power are discussed. Simulations are used to explain the results of implementing each control strategy. The performance of the proposed compensator is associated with the results of MATLAB/Simulink simulations.

III.METHODOLOGY

Using a wind-solar hybrid system with UPFC, the proposed model uses a PID controller to regulate the fact device and a PSO approach to establish the Kp and ki parameters. Mismatches in power generation and load power produce fluctuations in power supply voltage and frequency because renewable energy is by definition intermittent.

Grid-connected hybrid renewable energy systems, such as photovoltaic-wind, can be controlled using the unified power flow controller (UPFC). The proposed tuning technique is intended to assist address some of the shortcomings of the typical P&O MPPT tuning algorithm, such as oscillations at the maximum power point (MPP) and delayed convergence. Investigate MPP behavior in response to a variety of unpredictable and fast changing environmental conditions. The parameters of P&O MPPT controllers can be optimized utilizing a PSO-based technique.

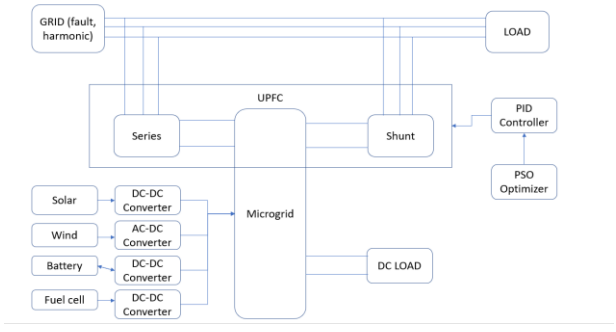

Fig 1. Proposed Block Diagram.

Because of the system's non-linearity and wide range of parameters, it is difficult to utilize standard tuning processes to set the controller to achieve optimum performance when using the PV system's P&O MPPT. The suggested control technique maintains a constant voltage variation while minimizing power losses. Using the PSO controller in conjunction with the PSO method to determine the optimal PI-C settings for UPFC improves the transient stability of the system. Each particle is composed of two Ki, Ki components. As a result, the search issue area has two dimensions, and each team member must fly in a two-dimensional environment. A critical stage in the use of PSO is selecting the fitness function to be used to evaluate the suitability of each particle.

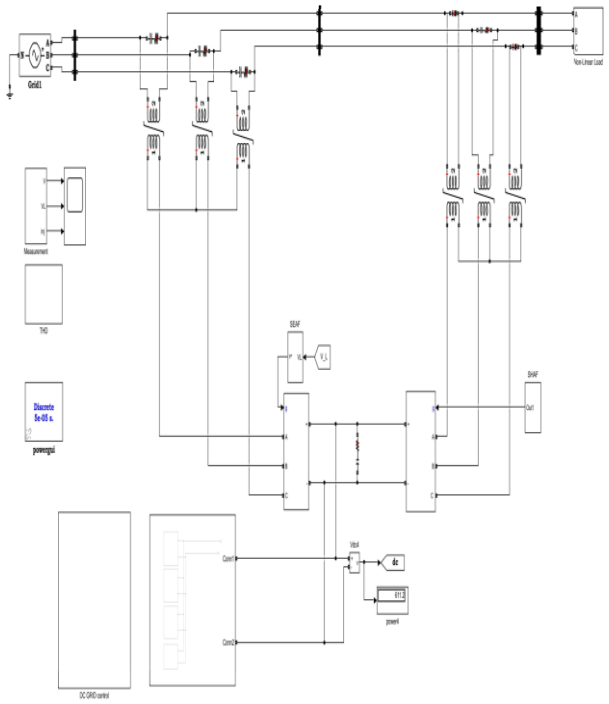

Fig 2. Proposed Simulink model.

1. Modules:

- Solar System
- Wind turbine
- PSO
- Battery
- Fuel cell
- Grid
- UPFC
- Fuzzy Controller

According to the study's findings, grid-connected hybrid renewable energy systems use power flow regulation. As a result, control methods for data collection must be developed in order to maximize the potential of a realistic network.

The UPFC is the most promising device for load flow control among flexible alternating current transmission system devices due to its capacity to regulate active and reactive power flow near the lines regardless of nodal voltages. According to the UPFC features, scheduling executions comprises a plethora of practical criteria in order to select the best site. In actuality, the best location for the UPFC is uncertain, and as a result, thorough study is rarely undertaken.

As a result of these disruptions, electrical equipment malfunction, have a shorter lifespan, and fail. When photovoltaic and wind energy systems are linked into the grid, power quality challenges such as harmonics, heat, and other complex power quality issues develop.

As a result, system efficiency suffers, as do transformer overheating and other issues. Effective current harmonic and power quality mitigation measures are essential to ensure the reliability of a renewable grid-connected system. Many remedies to these power quality challenges have been offered, including balancing loads, harmonic injection, and imbalanced systems.

Historically, grid-integrated systems were protected from series harmonics by utilising filters in conjunction with passive filters. These considerations contribute to the quick degradation of passive components, limiting the use of passive filters to a few applications. These concerns include: limited filtering; a limited load range; fixed compensation; a bigger diameter; negative resonance between grids; and filter impedance.

2. Control strategy of UPFC with proposed technique:

A system-based UPFC operation and control approach The performance of the UPFC is strongly reliant on the direct current link voltage being kept under control. Under dynamic system conditions such as unexpected changes in load and voltage sag, the direct current link feedback controller seeks to restore the direct current link voltage to the prescribed value as soon as possible. The UPFC's shunt and series active power filters allow it to manage both the source voltage and the load

current. The novel method simplifies the transmission of control signals to shunt and series active power filters.

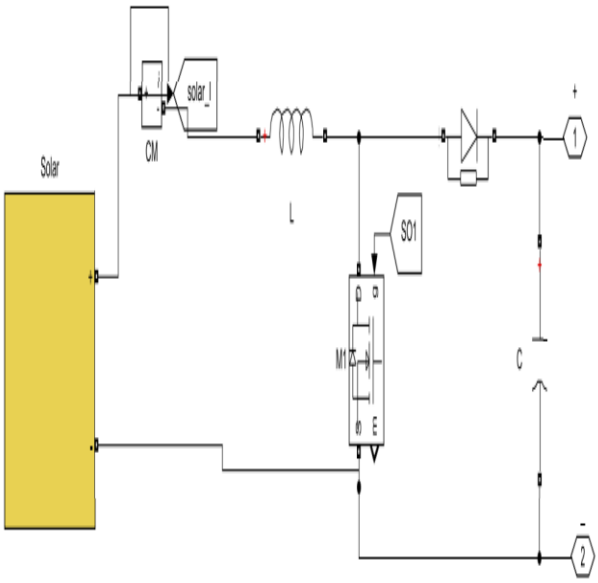

Fig 3. Solar subsystem.

This block models a solar cell as a parallel combination of a current source, two exponential diodes and a parallel resistor, Rp, that are connected in series with a resistance Rs.
The output current I is given by:

$$I = Iph - Is*(e^{((V+I*Rs)/(N*Vt))-1}) - Is2*(e^{((V+I*Rs)/(N2*Vt))-1}) - (V+I*Rs)/Rp$$

Where Is and Is2 are the diode saturation currents, Vt is the thermal voltage, N and N2 are the quality factors (diode emission coefficients) and Iph is the solar-generated current. Models of reduced complexity can be specified in the mask. The quality factor varies for amorphous cells, and typically has a value in the range of 1 to 2. The PS input Ir is the irradiance (light intensity) in W/m^2 falling on the cell. The solar-generated current Iph is given by Ir*(Iph0/Ir0) where Iph0 is the measured solar-generated current for irradiance Ir0.

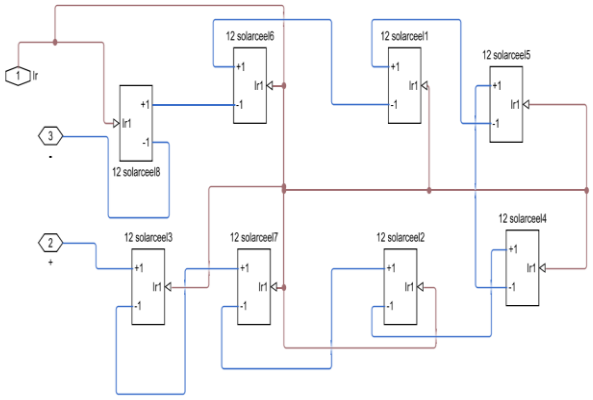

Fig 4. Solar cell block.

Table 1. Solar parameters.

Short-circuit current, Isc:	7.34
Open-circuit voltage, Voc:	0.6
Irradiance used for measurements, Ir0:	1000
Quality factor, N:	1.5

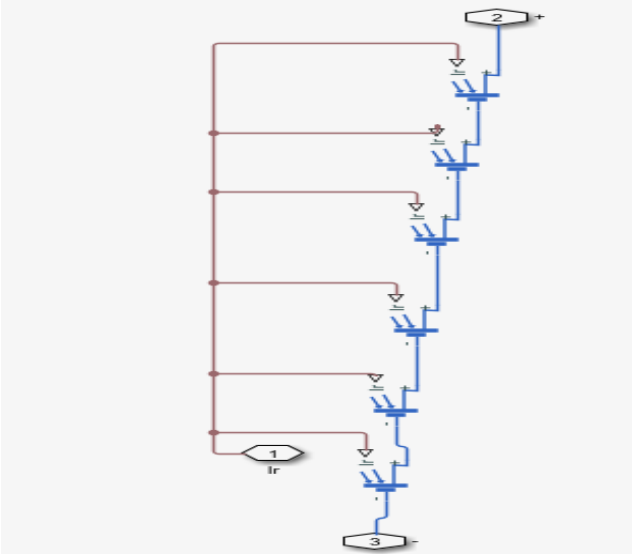

Fig 5.Solar Cell Array.

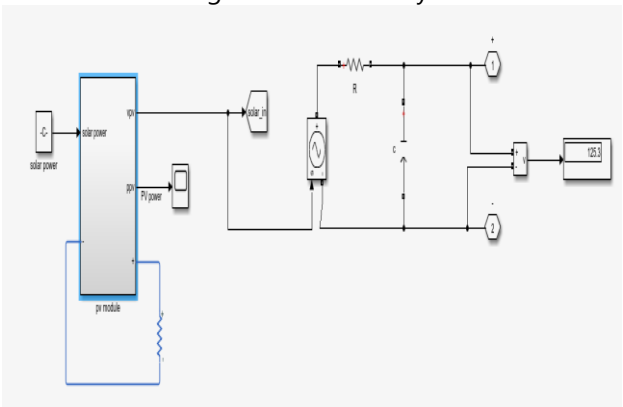

Fig 6. Solar Subsystem.

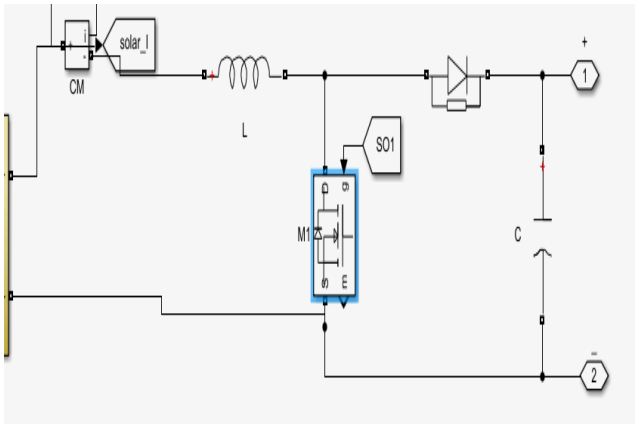

Fig 7. DC-DC boost converter.

MOSFET and internal diode in parallel with a series RC snubber circuit. When a gate signal is applied the MOSFET conducts and acts as a resistance (Ron) in both directions. If the gate signal falls to zero when current is negative, current is transferred to the antiparallel diode.

Table 2. Boost converter MOSFET configuration.

Parameters	Value
FET resistance Ron (Ohms) :	0.1
Internal diode resistance Rd (Ohms) :	0.01
Snubber resistance Rs (Ohms) :	1e5

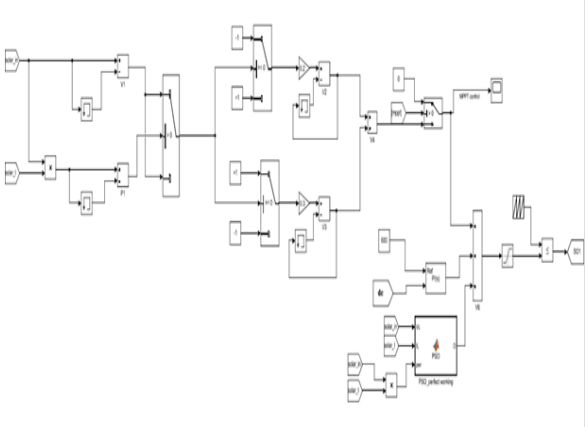

Fig 8. MPPT and PSO subsystem.

Maximum power point tracking, or MPPT, is an algorithm that continuously changes the impedance measured by a photovoltaic system under changing conditions to guarantee that the PV system is as near to the photovoltaic system in terms of performance and efficiency as possible.

3. MPPT Simulation Result of Perturb and Observation :

Perturb and Observe method is the most commonly used method for solar and wind energy conversion systems. In a solar PV system, the PV output voltage and current are measured two consecutive intervals. The power is calculated for two successive intervals. The change of power to change voltage is calculated dP/dV. Based on the positive and negative values of the slope dP/dV, the duty cycle is incremented or decremented.

Accordingly, the voltage and power are adjusted to the maximum PowerPoint. If the slope dP/dV=0, then the maximum power point is reached for the present environmental conditions. This is a continuous process. The measurements are to be continuously taken, and change power and voltage change are calculated to take control actions. The MPP is achieved by making the impedance of the solar PV with the impedance of the load side. The duty cycle is adjusted to match the impedance. This MPPT algorithm is explained in the previous chapter with a flow chart and algorithm. The algorithmic steps are given below.

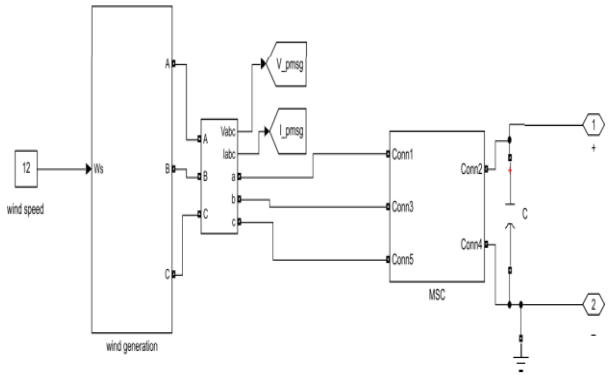

Fig 9. Wind subsystem.

Wind - This block's wind turbine type features a variable pitch. In terms of turbine efficiency, the Cp coefficient quantifies how much mechanical output power the turbine generates in relation to the amount of wind power (beta). Cp achieves its highest value at beta=0. Choose which wind-turbine power parameters you wish to examine on the graph, and then adjust the pitch angle to your liking.

The first parameter to be entered is the generator speed per unit of the generator's base speed. Asynchronous or asynchronous generators are built on the synchronous speed. A permanent-magnet generator's base speed is the rate at which nominal voltage is produced when no load is applied. The

second parameter is the blade pitch angle in degrees. The wind speed, measured in meters per second (m/s), is the third parameter. The output of the generator is measured in terms of torque applied to the shaft per unit of rated power.

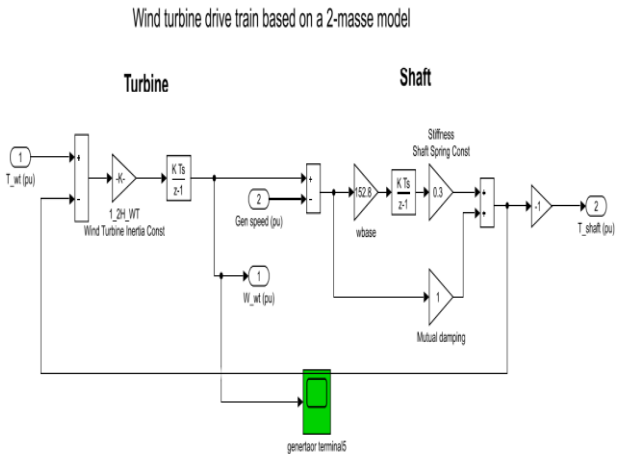

Fig10. turbine and shaft model.

The wind's energy turns the blades of a rotor, which look like propellers. The primary shaft connects the rotor to the generator, which spins in order to generate electricity. An electric wind system includes a wind turbine mounted on a tower. This enables it to benefit from stronger winds. In addition to the turbine and tower, small wind power systems require balance-of-system components.

4. Turbines:

The vast majority of small wind turbines on the market today are horizontal-axis upwind machines with two or three blades. These blades are frequently constructed from fibreglass or other composite materials. The turbine's structure is coupled to the rotor, generator, and exhaust pipe. The diameter of the rotor has the biggest effect on the amount of energy produced by a turbine.

The rotor diameter has an effect on the "swept area," or the quantity of wind gathered by the turbine. Due to the fact that wind speed increases with altitude, the tail assists in orienting the turbine in the direction of the wind towers. A miniature wind turbine is mounted to the tower's summit. Frequently, increasing the height of the towers increases the capacity of the wind system. Increasing the height of a tower in order to generate more electricity for a minor expenditure can have significant financial consequences.

While transporting power from a 60-foot to 100-foot tower costs 10% more, a 10-kilowatt generator now generates 25% more power. The majority of wind turbine manufacturers provide towers as an add-on to their wind energy systems. The most often used forms of towers in construction are self-supporting (or "free-standing") and guyed towers. Guyed towers are also available in tilt-down configurations. Due to the higher cost and difficulty of building self-supporting towers, guyed towers are frequently used in residential wind energy systems.

Because the guy radius must be half to three quarters the height of the tower to accommodate them, man-made structures demand more space than guyed structures.

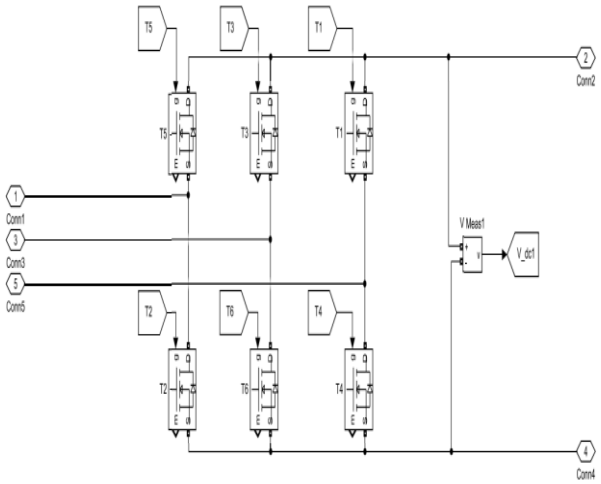

Fig 11. Multi-inverter ac to dc circuit for wind generation.

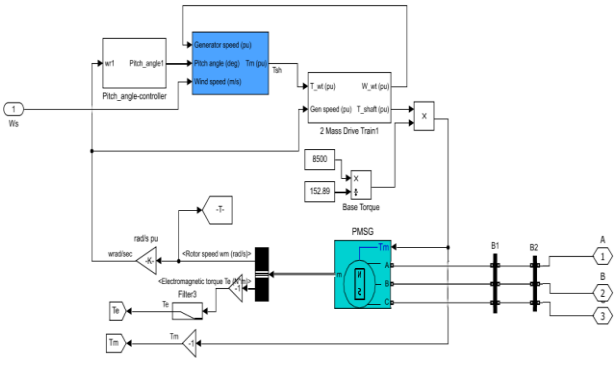

Fig 12. PMSG generator.

Implements a three-phase or a five-phase are permanent magnet synchronous machine. The stator windings are connected in wyes to an internal neutral point. The three-phase machine can have sinusoidal or trapezoidal back EMF waveform.

The rotor can be round or salient-pole for the sinusoidal machine, it is round when the machine is trapezoidal. Preset models are available for the Sinusoidal back EMF machine. The five-phase machine has a sinusoidal back EMF waveform and round rotor.

Table 3. PMSG generator parameters.

Parameters	Value
Stator phase resistance Rs (ohm):	0.425
Armature inductance (H):	0.000395
Flux linkage:	0.433
Inertia, viscous damping, pole pairs, static friction [J(kg.m^2) F(N.m.s) p() Tf(N.m)]:	[0.01197 0.001189 5]

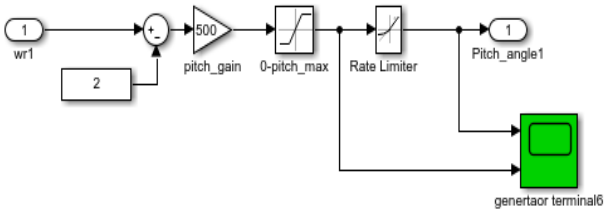

Fig 13.Pitch Angle Subsystem.

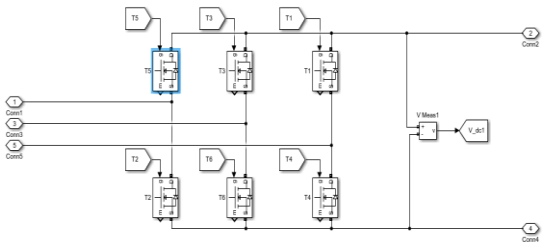

Fig 14.Inverter Subsystem for wind.

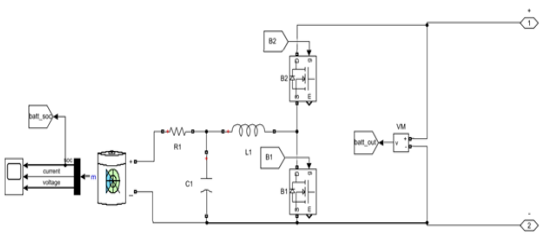

Fig 15. Battery Model.

A battery contains an electrochemical cell. Externally linked batteries can power items such as flashlights, cell phones, and electric cars. When the battery is functioning, the cathode is the positive terminal and the anode is the negative terminal. Electrons pass from the terminal with a negative mark to the positive electrode through an external circuit. An external load activates the battery's redox reaction, producing a low-energy byproduct. The free energy that has been lost is transformed to electrical energy and delivered outside the system. It used to refer to a device with several batteries, but the phrase has now come to refer to a device with a single battery.

Table 4. Battery parameters.

Parameters	value
Nominal voltage (V)	108
Rated capacity (Ah)	26
Initial state-of-charge (%)	97
Battery response time (s)	30
Maximum capacity (Ah)	26
Cut-off Voltage (V)	81
Fully charged voltage (V)	110.3807
Nominal discharge current (A)	22.3478
Exponential zone [Voltage (V), Capacity (Ah)]	[108.7788 27.2653]
Discharge current [i1, i2, i3,...] (A)	[6.5 13 32.5]

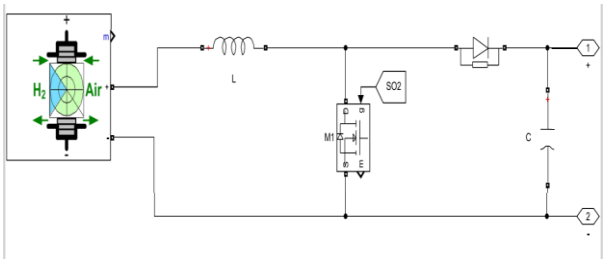

Fig16. Fuel cell model.

Table 5. Fuel cell parameters.

Parameters	Value
Voltage at 0A and 1A [V_0(V), V_1(V)]	[65,63]
Nominal operating point [Inom(A), Vnom(V)]	[133.3,45]
Maximum operating point [Iend(A), Vend(V)]	[225,37]
Number of cells	65
Nominal stack efficiency (%)	55
Nominal Air flow rate (lpm)	300

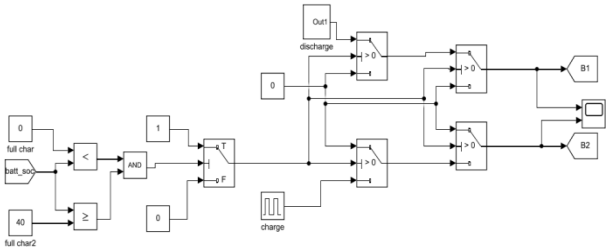

Fig 17. Battery subsystem.

The direct current bus voltage is managed via fuzzy logic control. However, fuzzy logic control requires a large amount of data. Particle swarm optimization is used to prevent the hybrid from growing excessively large as a result of its efficiency. However, particle swarm optimization has a limited potential for doing local searches. To address these challenges, a UPFC device built on cutting-edge technology and a control technique that is acceptable are required.

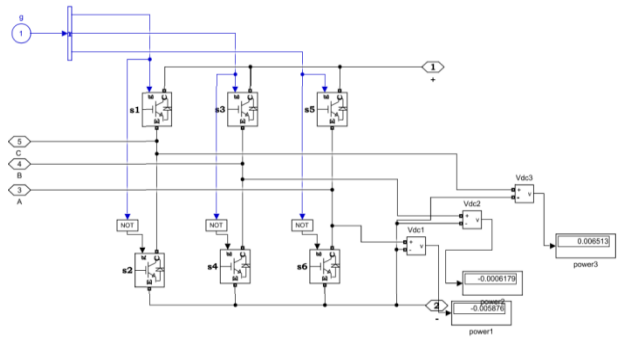

Fig 18. UPFC VSC Circuit.

Figure 18 depicts the UPFC, a hybrid STATCOM/SSSC system with a high degree of operational adaptability. The secondary winding of each transformer is connected to a three-phase voltage-source converter in this set-up. This allows power to be exchanged between shunt and series systems in either direction with adequate coordination between the control systems of the two converters when they are connected back-to-back as a direct current link with their direct current capacitors acting as a common direct current voltage source. Each converter also has the capability of supplying or absorbing Mvar to series or shunt systems on an individual basis.

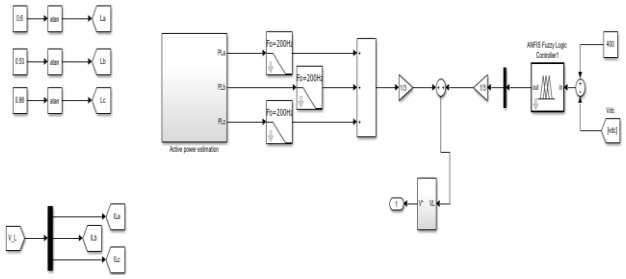

Fig19. ANFIS control.

5. Phase Locked Loop (PLL) –

This Phase Locked Loop (PLL) system can be used to synchronize on a set of variable frequency, three-phase sinusoidal signals. If the Automatic Gain Control is enabled, the input (phase error) of the PLL regulator is scaled according to the input signal magnitude.

For optimal performance, the following settings are recommended:

[Kp Ki Kd] = [180 3200 1]

"Enable Automatic Gain Control" checked
Input 1: Vector containing the normalized three-phase signals [Va Vb Vc]
Output 1: Measured frequency (Hz) = w/(2pi)
Output 2: Ramp w.t varying between 0 and 2*pi,
Synchronized on zero crossings of the fundamental (positive-sequence) of phase A.
Output 3: Vector [sin(wt) cos(wt)

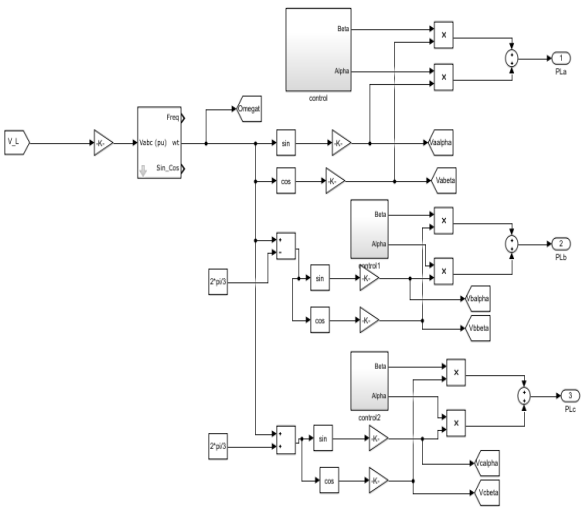

Fig 20. PLL Control Subsystem.

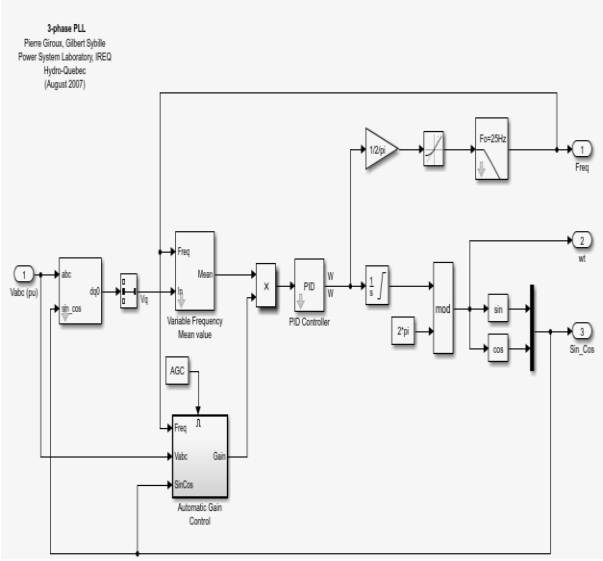

Fig 21. PLL Subsystem.

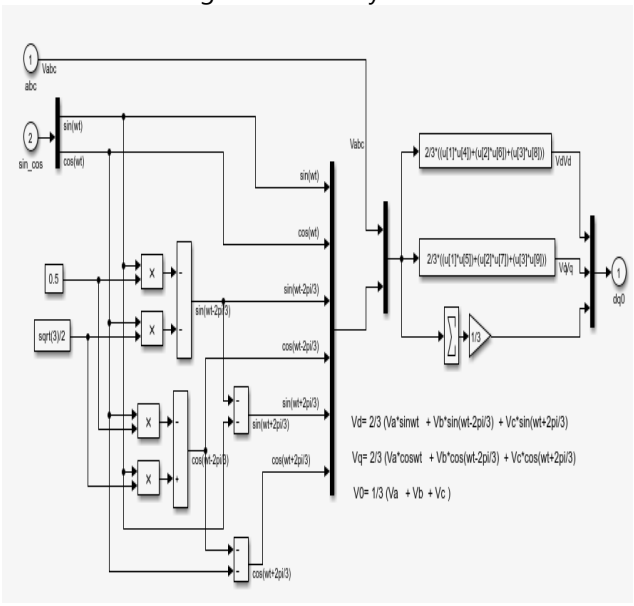

Fig 22.AGC Control System.

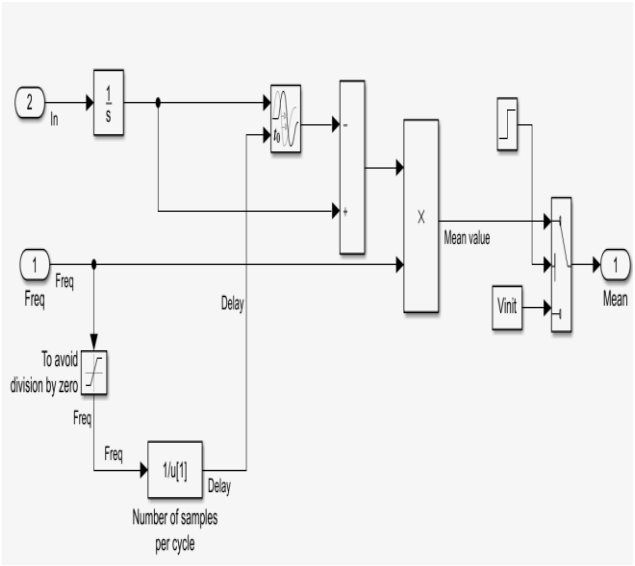

Fig 23. PLL Frequency Control Subsystem.

Apply a delay to the first input signal. If the delay type is variable time delay, the second input specifies the delay time To. The block implements the function y=u(t-To(t)). If the delay type is variable transport delay, the second input specifies the instantaneous delay time Ti at the input.

The block can be used to simulate the variable transport delay phenomenon such as incompressible liquid flow in a pipe.

Best accuracy is achieved when the delay is larger than the simulation step size. Convert the input to the data type and scaling of the output.The conversion has two possible goals. One goal is to have the Real World Values of the input and the output is equal. The other goal is to have the Stored Integer Values of the input and the output is equal. Overflows and quantization errors can prevent the goal from being fully achieved.

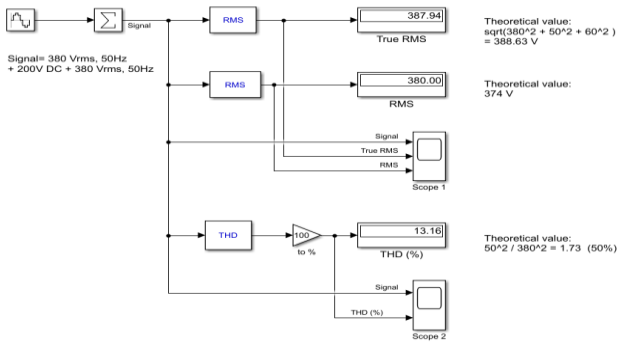

Fig 24. THD Block.

6. Simulation results:

The proposed technique, on the other hand, is discussed in this part, together with the simulation results and power flow management. The proposed approach is simulated using the MATLAB software platform.

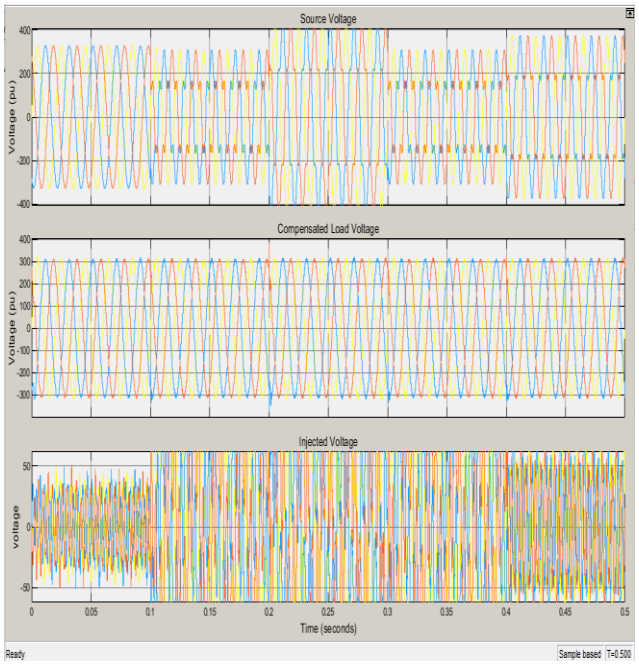

Fig25. Source, compensated voltage and injected voltage waveform.

Figure 25 displays the voltage sag simulation from 0 to 0.5 seconds. Throughout this time period, the DVR will inject the required voltage,. Following the adjustment, the load voltage is shown in fig.25

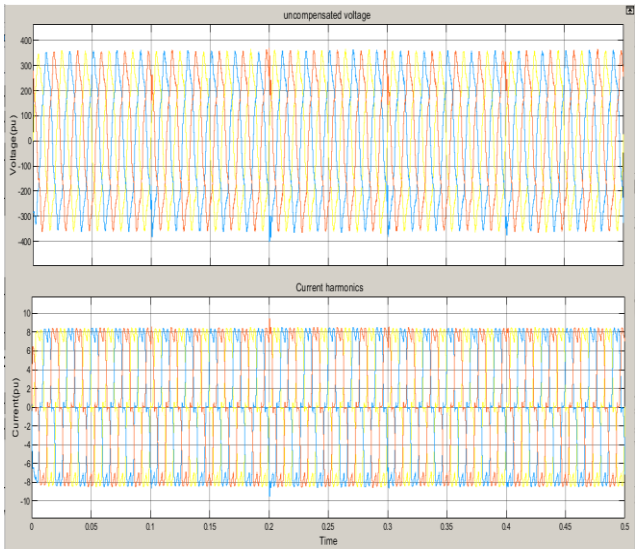

Fig26. Compensated voltage and current harmonics wave form.

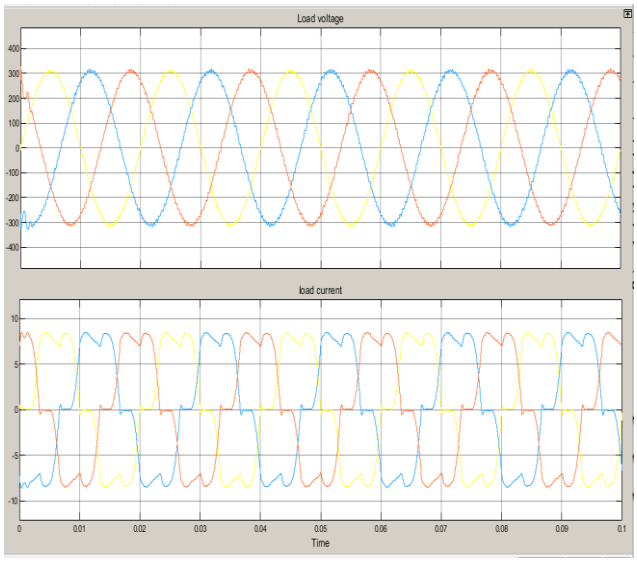

Fig 27. Load voltage and load current waveform.

The voltage sag is simulated between 0 and 0.5 seconds, as illustrated in fig 27 During this time period, DVR will inject the required voltage, as illustrated in Figure 6. The load voltage is as shown in fig 27 after correction.

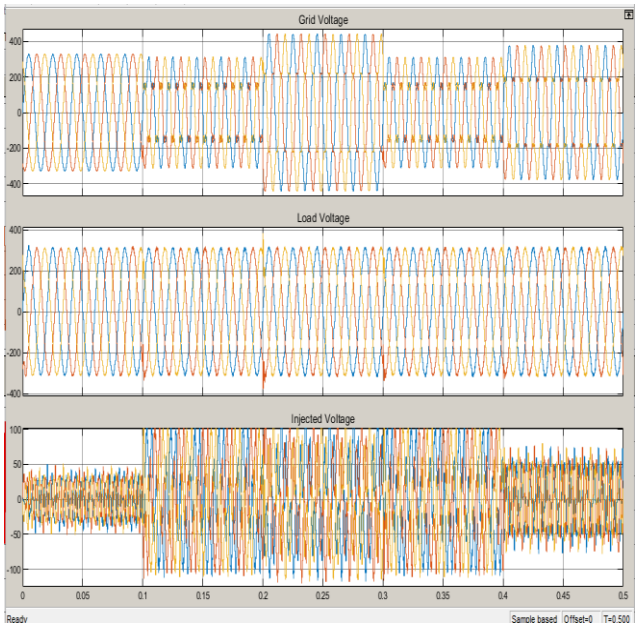

Fig 28. Grid voltage, load voltage and injected voltage waveform.

The control techniques for a synchronous reference frame-based DVR were modeled in MATLAB Simulink, and their performance under various grid circumstances was evaluated. The voltage swell, sag, and harmonics are reproduced between 0 and 0.5

seconds, when the DVR injects the needed voltage. Following adjustment, the load voltage is displayed.

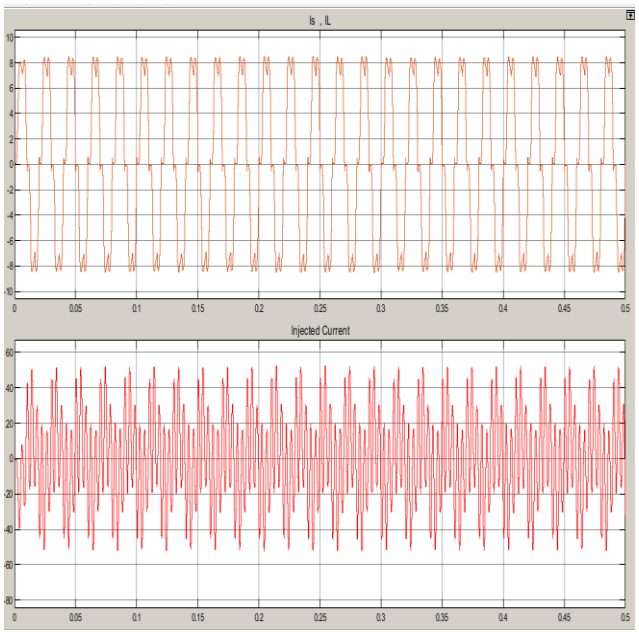

Fig 29. Injected current and load current waveform.

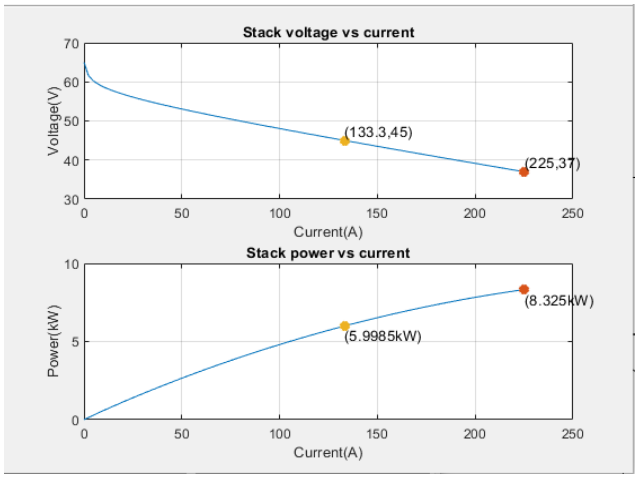

Fig 30. Fuel Cell Characteristics.

Table 6 THD comparison result with existing work

Parameters	Techniques	THD (%)
Load Voltage	Modified D-STATCOM	9.37
RMS Current		7.66
Load Voltage	UPFC	1.96
RMS Current		1.73

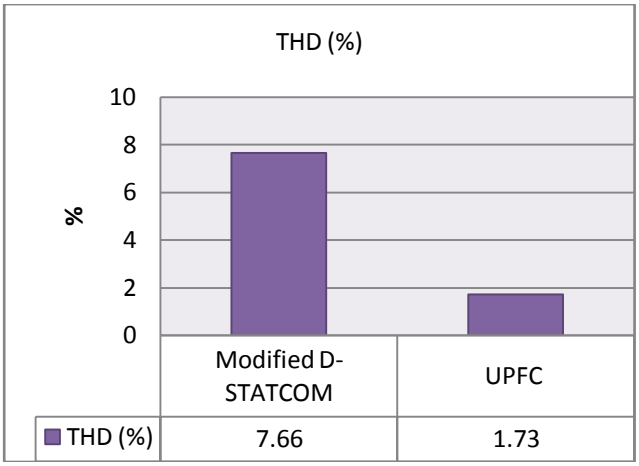

Fig 31. THD result performance for load Current

IV. CONCLUSIONS

The proposed way of incorporating the UPFC in the power system's transmission line outperforms older technologies such as the power system stabilizer and automated voltage controller. Implementing a UPFC increases transient stability since it can compensate in both series and shunt modes.

A UPFC provides higher transient stability performance. According to the power flow management strategies developed for the systems and power consumption by load, the controller performs well and also achieves the system's power balance, as proved by the simulation of a UPFC-equipped hybrid renewable energy system in this thesis. According to the simulation results, the power generation of the photovoltaic-wind system always matches the demand of the system's load. According to the results of the MATLAB simulation, the proposed technique was viable and had a lot of potential. We discovered a solution to the significant power fluctuation in a grid-connected system. As a result, the algorithm's complexity can be lowered while still identifying the best solution.

Other flexible alternating current transmission system components may be used in the future to replace the UPFC. Power quality events like voltage sag and swell can be included in a stability study. With the use of controllers, hybrid systems may be built to explore the dynamic and stable features of network-connected systems, such as photovoltaic wind, wind fuel cell, wind diesel, wind hydro and wind-photovoltaic diesel-fuel cell-hydro. To get a

good range of values for the gains Kp and KI, we must go through several simulations and iterations. As a result, adjusting the PI controller gain settings has proven difficult. An optimization framework may be built to calculate Kp and KI values, which will lead to an upfc that performs better overall. In addition, the UPFC's performance can be improved by switching from the fixed gain PI controller to one of many adaptive control methods.

REFERENCES

[1] Preeti Ranjan Sahu;Prakash Kumar Hota;Sidhartha PandaComparison of Grasshopper and Whale Optimization Algorithm for Design of FACTS Controller with Power System Stabilizer 2018 Fifth International Conference on Parallel, Distributed and Grid Computing (PDGC) Year: 2018.

[2] Ahmed Ashraf Abbas;Hossam Hassan Ammar;Mahmoud Mohamed Elsamanty Controller Design and Optimization of Magnetic Levitation System (MAGLEV) using Particle Swarm optimization technique and Linear Quadratic Regulator (LQR) 2020 2nd Novel Intelligent and Leading Emerging Sciences Conference (NILES) Year: 2020

[3] Mohammad Ali Daftari;Mohammad Ali Nekoui Analysing Stability of Time Delayed Synchronous Generator and Designing Optimal Stabilizer Fractional Order PID Controller using Partical Swarm Optimization Technique 2018 2nd IEEE International Conference on Power Electronics, Intelligent Control and Energy Systems (ICPEICES) Year: 2018

[4] Mahmoud F. Mahmoud;Ahmed T. Mohamed;Lobna A. Said;Ahmed H. Madian;Ahmed G. Radwan Power Tracking Controller Design For Photo-voltaic Systems Based On Particle Swarm Optimization Technique 2019 31st International Conference on Microelectronics (ICM) Year: 2019.

[5] P Amritansh Naidu;Varsha Singh Speed control of induction motor and control of multilevel inverter output with optimal PI controller using DE and GSA optimization technique 2018 3rd International Conference on Communication and Electronics Systems (ICCES) Year: 2018.

[6] Nimai Charan Patel;Manoj Kumar Debnath;Binod Kumar Sahu;Subhransu Sekhar Dash;Ramazan Bayindir Multi-Staged PID Controller Tuned by Invasive Weed optimization Algorithm for LFC Issues 2018 7th International Conference on Renewable Energy Research and Applications (ICRERA) Year: 2018.

[7] Ramesh Devarapalli;Biplab Bhattacharyya Application of Modified Harris Hawks Optimization in Power System Oscillations Damping Controller Design 2019 8th International Conference on Power Systems (ICPS) Year: 2019.

[8] Anjali Atul Bhandakkar;Lini Mathew Optimal placement of unified power flow controller and hybrid power flow controller using optimization technique 2018 IEEE/IAS 54th Industrial and Commercial Power Systems Technical Conference (I&CPS) Year: 2018.

[9] Sajid Hussain Qazi;M.A Uqaili;U Sultana Whales Optimization Algorithm Based Enhanced Power Controller for an Autonomous Microgrid System 2019 8th International Conference on Modern Power Systems (MPS) Year: 2019.

[10] Subhasis Bando padhyay;A. Bandyopadhyay Harmonics Elimination in 24 Pulse GTO Based STATCOM by Fuzzy Logic Controller with Switching Angle Optimization using Grey Wolf Optimizer 2020 IEEE 5th International Conference on Computing Communication and Automation (ICCCA) Year: 2020.

[11] Akshay Sunil Vikhe;A. A. Kalage Power System Optimization using Ant Lion Optimisation Technique 2019 3rd International conference on Electronics, Communication and Aerospace Technology (ICECA) Year: 2019.

[12] Soham Dey;Jayati Dey;Subrata Banerjee Optimization Algorithm Based PID Controller Design for a Magnetic Levitation System 2020 IEEE Calcutta Conference (CALCON) Year: 2020.

[13] Anderson, P.M., Faud, A.A, Power system control and stability. Galgotia Publication, 1981.

[14] Concordia, C., "Effect of steam turbine reheat on speed-governor performance." ASME J. Eng.Power, Volume- 81, (1959):pp.201-206,.

[15] Kirchmayer, L.K., Economic Control of Interconnected Systems, Wiely, NewYork, 1959.

[16] Young, C.C., and Webler R.M., "A new stability program for predicting the dynamic performance of electric power systems", Proc. Am. Power Conf., Volume-29, (1967): pp.1126-1139.

[17] Byerly, R.T, Sherman D.E., Stability program data preparation manual. Westinghouse Electric Corp., 1970.

[18] Crary S.B., Power System Stability, Volume.2, Wiely, New York, 1947.

[19] Ewart, D.N., Flexible AC transmission systems (FACTS) scoping study, 1990.

[20] Hingorani, N.G.: 'High power electronics and flexible AC transmission system', IEEE Power Eng. Reo., July 1988.

[21] Maliszewski, R.M., Power flow in highly integrated transmission network, CIGRE, 1990 [10]Christl, N. Advanced series compensation with variable impedance, EPRI Workshop onFACTS, Cincinnati, Ohio, USA, November 1990.

[22] Gyugyi, L., "Reactive power generation and control by Thyristor circuits", IEEE Trans.Ind. Appl., (1979).

[23] Sumi, Y., "New static VAr control using force-commutated inverters", IEEE PES Winter Power Meeting, Volume 38 (1981).

Gyugyi, L., "Advanced static VAr compensator using @le turn-off thyristors for